IOP PUBLISHING JOURNAL OF PHYSICS: CONDENSED MATTER

J. Phys.: Condens. Matter **19** (2007) 116105 (10pp) doi:10.1088/0953-8984/19/11/116105

Liquid polymorphism, density anomaly and H-bond disruption in associating lattice gases

Aline Lopes Balladares[1], **Vera B Henriques**[2] **and Marcia C Barbosa**[1,3]

[1] Instituto de Fisíca, Universidade Federal do Rio Grande do Sul, Caixa Postal 15051, 91501-970, Porto Alegre, RS, Brazil
[2] Instituto de Física, Universidade de São Paulo, Caixa Postal 66318, 05315970, São Paulo, SP, Brazil

E-mail: marcia.barbosa@ufrgs.br

Received 14 September 2006, in final form 28 January 2007
Published 5 March 2007
Online at stacks.iop.org/JPhysCM/19/116105

Abstract

We have investigated the effects of either distorting hydrogen bonds or removing proton degeneracy on the thermodynamic properties of a minimal model for associating liquids. The presence of two liquid phases and a density anomaly is unaffected in both cases. Increasing the degeneracy of bonded structures leads to lower-temperature critical points and a steeper liquid–liquid coexistence line, implying a low-density liquid of larger entropy.

Analysis of the hydrogen-bond net across the phase diagram indicates that the density anomaly is accompanied by a steep reduction of hydrogen-bond density, which introduces a restriction on a correlation which was precognized long ago. This feature is present independent of bond distortion or of the presence of proton entropy.

1. Introduction

Network-forming liquids such as water are ubiquitous [1] in nature. They differ from normal liquids by the presence of directional intermolecular interactions that result in the formation of bonds. These directional attractive forces favour the formation of structured regions that, due to the orientational constraints on the bonded molecules, have lower density than non-bonded regions. As a result, a density anomaly, consisting in the expansion under isobaric cooling of these systems, appears. This density anomaly has been related to a phase transition between a low-density liquid (LDL) and a high-density liquid (HDL). Experiments and simulations of water predict a HDL–LDL first-order phase transition in an experimentally inaccessible region of the phase diagram [2–6]. But water is not an isolated case, computer simulations of phosphorus [9], SiO_2 [10], and Si [11, 12] suggest the existence first-order LDL–HDL phase

[3] Author to whom any correspondence should be addressed.

0953-8984/07/116105+10$30.00

transitions in these materials. In the case of carbon the literature shows both evidences of the presence [7] and of the absence [8] of two liquid phases.

The presence of a number of solid phases in water, as well as of solid–solid first-order phase transitions, have suggested the possibility that systems with solid polymorphism exhibit several liquid phases with local structures similar to the ones present in the crystal phases. This assumption was confirmed for a number of polymorphic liquids such as Se, S, Bi, P, I_2, Sn, Sb, As_2Se_3, As_2S_3 and Mg_3Bi_2 [13, 14].

In all these cases, a full understanding of the effects of the number, spatial orientation and strength of the bonds is still missing. In order to shed some light onto this problem, recently a simple approach representing hydrogen bonds through ice variables [15–18] has been proposed. The zero-temperature ice model was successful in giving the description of ice [19] entropy for dense systems, but an order–disorder transition for finite temperatures is absent. Recently, a description based also on ice variables but which allows for a low density ordered structure [20, 21] was proposed. The associating lattice gas model (ALG) [20, 21] is based on the competition between the filling up of the lattice and the formation of an open four-bonded orientational structure which is naturally introduced in terms of the ice bonding variables and no ad hoc introduction of density or bond strength variations is needed. In our previous publications, we have shown that this model is able to exhibit, for a convenient set of parameters, both density anomalies and the two liquid phases [20]. It was also shown that by varying the relative strength of the orientational interaction we can go at a fixed temperature from two coexisting liquid phases, as observed in amorphous water, to a smooth transition between two amorphous structures, as might be the case of silica [21].

In the case of water, in the region of the pressure versus temperature (p–T) phase diagram where the density anomaly is present, the presence of distorted hydrogen bonds, which favour the presence of interstitial non-bonded water molecules has been reported [23]. These non-bonded molecules weaken the actual bonded interaction in their vicinity.

On the other hand, investigations on orientational models without distinction between donor and acceptor arms [22] pose the question of whether this distinction, essential in the case of the original ice entropy problem [19], has any effect on some of the important anomalous properties one aims to represent.

In this study we firstly wish to contribute to the search for a minimum model for anomalous associating liquids, in establishing which of the microscopic properties are essential in order to reproduce the macroscopic behaviour expected for water. We propose to analyse two features: (i) the presence of distorted bonds and (ii) the absence of proton entropy on bonds.

A second purpose of our work is to look for the correlations between hydrogen-bond behaviour and the density anomaly. The water density anomaly has for a long time been associated with bond breaking or bond distortion [24]. As temperature is increased, bonds break or distort and allow an increased number of neighbours per molecule. As temperature increases further, the usual translation entropy dictates dilution, and the more usual reduction in density prevails. However, it is well known that the TMD line (line of maximum density) is restricted to some range of pressures, in the vicinity of the liquid–liquid line. This means that pressure is required to play a role in inducing an increase in density as temperature rises. In this study we also aim at analysing the relation between bond-breaking and rising density as functions of temperature.

The remainder of the paper goes as follows. In section 2, the model for distorted hydrogen bonds is introduced and the corresponding phase diagrams are obtained. In section 3, a simplified version of the original associating lattice gas model in which the distinction between donors and receptors is removed is presented and its properties compared with those of the

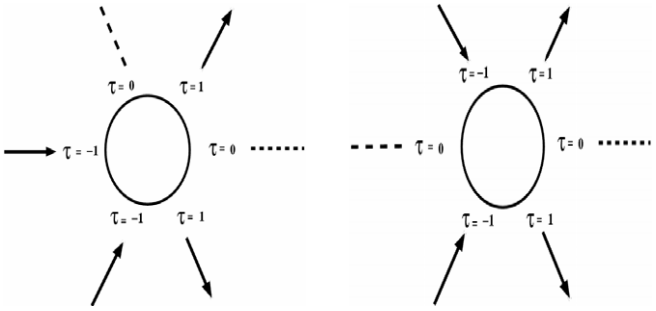

Figure 1. The model orientational state: four bonding (donor and receptor) and (a) two distorted non-bonding arms and (b) two opposite arms.

original asymmetric model. Results for the hydrogen-bond densities are presented in section 4. Finally, conclusions are presented in section 5.

2. The distorted-bond associating lattice gas model

Consider a two-dimensional triangular lattice where each site may be empty or full. Associate with each site two kinds of variables: occupational variables, σ_i, and orientational variables, τ_i^{ij}. The orientational state of particle i is defined by the configuration of its bonding and non-bonding arms, as illustrated in figure 1. We consider three possible values for the ij arm variables. Four are the usual ice bonding arms, two donor ($\tau_i^{ij} = 1$) and two acceptor ($\tau_i^{ij} = -1$), and two additional arms are taken as inert or non-bonding ($\tau_i^{ij} = 0$). A bond is formed if a donor arm points to a nearest neighbour acceptor arm. Bonding arms can be 'proper' or 'distorted'. Proper bonding is considered for the cases in which the non-bonding arms are opposite, as in figure 1(b). Bonds may be distorted if the non-bonding arms make an angle of 120°, as shown in figure 1(a). Thus there are three proper bonding states and six distorted bonding states per particle, making up 54 possible states per occupied site.

An energy $-v$ is attributed to each pair of occupied neighbouring sites that form a hydrogen bond if neither molecule has distorted arms, while non-bonding pairs are attributed an energy of $-v + 2u_1$. If at least one of the two molecules has a distorted bonding arm, the energy of the pair is given by $-v+2u_1-2u_2$. This makes $-2u_1$ the energy of proper hydrogen bonds whereas $-2u_2$ is the energy per bond of molecules in the distorted local net. The penalty for distortion is thus $2(u_1 - u_2)$.

The overall model energy is given by

$$E = (-v + 2u_1) \sum_{(i,j)} \sigma_i \sigma_j + \sum_{(i,j)} u_{i,j} \sigma_i \sigma_j \tau_i^{ij} \tau_j^{ji} (1 - \tau_i^{ij} \tau_j^{ji}) \tag{1}$$

where $\sigma_i = 0, 1$ are the occupational variables and $\tau_i^{i,j} = 0, \pm 1$ represents the arm states described above. As for H-bonds, described by the parameters $u_{i,j}$, we have $u_{i,j} = u_1$ if both molecules at sites i and j have opposite non-bonding arms, whereas $u_{i,j} = u_2$ if at least one of the two molecules i and j is distorted. Note that each particle may have six neighbours, but the number of bonds per molecule is limited to four.

This system can exhibit a number of ordered states. Two of them, without distorted bonds, are illustrated in figure 2. In figure 2(a) a fully occupied system with each molecule making four hydrogen bonds is shown. This is the high-density liquid phase. Figure 2(b) illustrates the

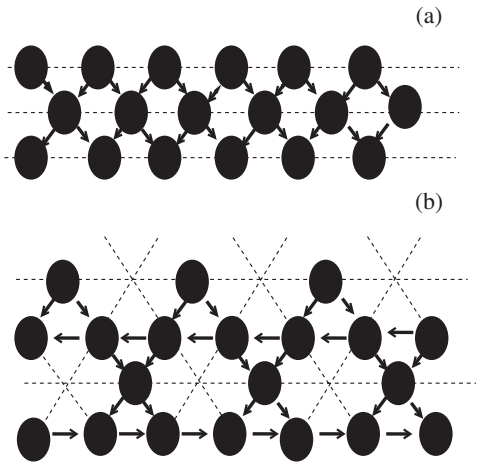

Figure 2. High-density liquid, HDL, with unit density (top) and low-density liquid, LDL, with density three-quarters (bottom) on the triangular lattice. The solid lines indicate the hydrogen bonds where the arrows differentiate bond donors from bond acceptors.

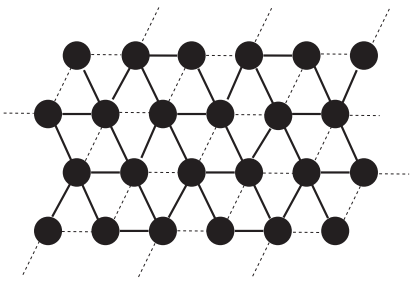

Figure 3. A possible configuration if the system could have all sites distorted. The solid lines indicate the hydrogen bonds and the dashed lines are the non-bonding interactions.

configuration in which the system has three-quarters of its sites occupied and each site has four hydrogen bonds. This is the low-density liquid phase. In both cases, none of the molecules is distorted and the energies per site are given by $e = -3v + 2u_1$ and $e = -3v/2$ respectively. Another low-energy configuration, with distortions, is illustrated in figure 3. In this case, the system is fully occupied, with all molecules making four hydrogen bonds; however, differently from the configuration in figure 2(a), all molecules are distorted and the energy per site is $e = -3v + 6u_1 - 4u_2$.

At zero temperature, the phase diagram is obtained simply by comparing the grand potential per site of the different configurations. Here we will assume that $u_1 > u_2$ so that the distortion is punished by having a higher energy. Thus, at high chemical potential, the lowest grand potential per site is the one of the high-density liquid phase without distortions ($\rho = 1$), illustrated in figure 2(a), $\phi_{hdl} = -3v + 2u_1 - \mu$. As the chemical potential is decreased, the low-density liquid ($\rho = 0.75$) without distortions with the grand potential per site given by $\phi_{ldl} = -3v/2 - 3\mu/4$ becomes energetically more favourable and, at $\mu = -6v + 8u_1$, there is a transition between a high-density liquid and a low-density liquid. Similarly, the pressure of coexistence between the two liquid phases at zero temperature is given by $p = -3v + 6u_1$.

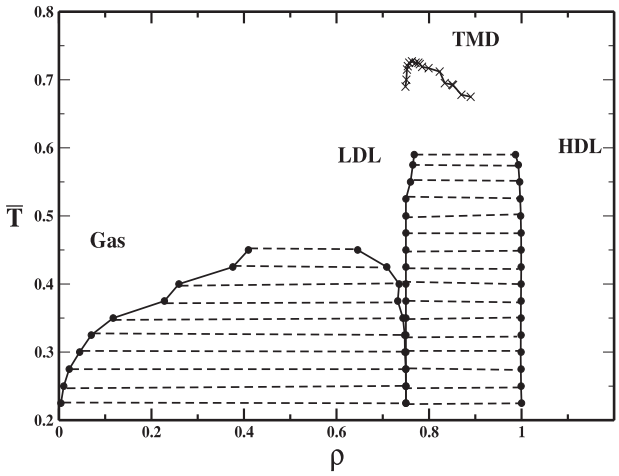

Figure 4. Temperature versus density coexistence phase diagram for $u_2/v = 0.6$. The two liquid phases, the gas phase and the temperature of maximum density are illustrated.

If the chemical potential decreases even further, the gas phase with $\phi_{\text{gas}} = 0$ becomes energetically more favourable and at $\mu = -2v$ and $p = 0$ there is a phase transition between a low-density liquid phase and a gas phase. The condition for the presence of the two liquid phases is therefore $u_1/v > 0.5$. For lower values of $u_1/v > 0.5$, the LDL disappears.

The model properties for finite temperatures were obtained through Monte Carlo simulations in the grand-canonical ensemble using the Metropolis algorithm. Some test runs were done for $L = 10$, 20 and 50. A finite size scaling analysis for the two critical temperatures shows a small shift not relevant for our analysis. Therefore, the detailed study of the model properties and the full phase diagrams was undertaken for an $L = 10$ lattice. Runs were of the order of 10^6 Monte Carlo steps.

We have considered the cases $u_1/v = 1$ for proper bonds and $u_2/v = 0.6$, 0.8 for distorted bonds. Figure 4 illustrates the reduced temperature, $\bar{T} = k_{\text{B}}T/v$, versus density coexistence phase diagram for $u_2/v = 0.6$. The low-density liquid phase occurs in a very small interval of densities, related to a very steep rise in the chemical potential isotherms. The line of maximum densities (TMD) is also shown in the figure.

Pressure was calculated by numerical integration of the Gibbs–Duhem equation at fixed temperature, from zero pressure at zero density. Figure 5 shows the $\bar{p}$–$\bar{T}$ ($\bar{p} = k_{\text{B}}p/v$) phase diagram for both $u_2/v = 0.6$ and $u_2/v = 0.8$. Data for the non-distorted version of the associating lattice gas model [20, 21] are also shown for comparison. The two coexistence lines, HDL–LDL and LDL–gas, and the TMD line are present, but displaced, if compared with the non-distorted case.

What is the effect of the hydrogen-bond distortion? Both critical points for the model without distortions are at higher temperatures when compared with the case in which distortions are allowed, as shown in table 1. The high degeneracy of the distorted bond model smoothens the LDL–HDL transition, thus destroying the transition, whereas it would still be present if the distortions were forbidden. The large degeneracy of the distorted bond molecules is also responsible for the larger slope of the LDL–HDL coexistence line near the critical point. This slope is positive, indicating, according to the Clapeyron condition, a more entropic LDL phase, if compared with the HDL phase. According to the same condition, the slope of this line is proportional to the variation of entropy upon the change of phase. This implies that the

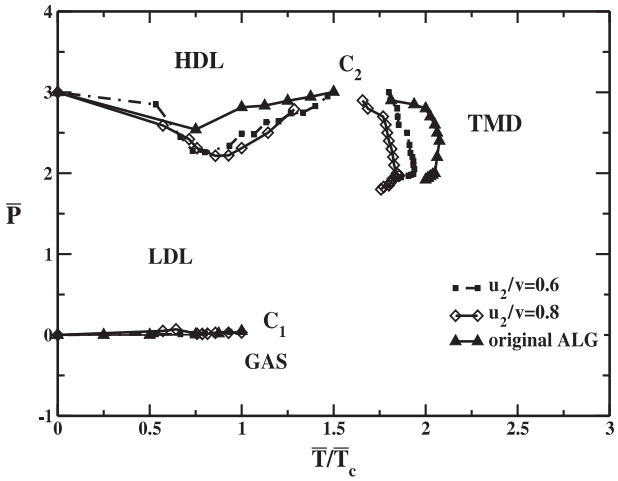

Figure 5. Reduced pressure versus reduced temperature for $u_2/v = 0.6, 0.8$. The temperatures are measured in terms of the LDL–gas critical point of each system. The original ALG data are also shown for comparison. The error bars are not shown for clarity.

Table 1. Reduced temperature, chemical potential and pressure at the two critical points for the original model, distorted and symmetric models.

System	$\bar{T}_{c1}$	$\bar{\mu}_{c1}$	$\bar{P}_{c1}$	$\bar{T}_{c2}$	$\bar{\mu}_{c2}$	$\bar{P}_{c2}$
Original ALG	0.45	−2.05	0.1792	0.65	1.71	3.005
$u2/v = 0.6$	0.375	−2.09	0.04	0.575	1.76	2.95
$u2/v = 0.8$	0.375	−2.09	0.03	0.45	1.48	2.70
Symmetric	0.55	−1.86	0.07	0.825	2.02	3.06

difference in entropy between the two phases is larger for the case of distorted bonds, implying a higher entropy LDL phase for the distorted as compared with the non-distorted case.

From table 1 we also observe that the critical temperatures for $u2/v = 0.6$ are closer than for $u2/v = 0.8$ to the critical temperatures of the original model. The case $u2/v = 0.8$ represents a lower energy for the distorted bonds than the case $u2/v = 0.6$; consequently, more distorted configurations are accepted for $u2/v = 0.8$ than for $u2/v = 0.6$.

3. The symmetric-arm associating lattice gas model

In order to test the relevance of proton distribution entropy with respect to the phase diagram properties, we study a third version of our model. In this version we do not distinguish the acceptor and donor arms, as illustrated in figure 6. Distorted bonds are forbidden. Under this approach the model is considerably simplified and only three orientational states per particle remain. The overall energy is given by

$$E = (-v + 2u) \sum_{(i,j)} \sigma_i \sigma_j + u \sum_{(i,j)} \sigma_i \sigma_j \tau_i \tau_j. \tag{2}$$

The $\bar{p}$–$\bar{T}$ phase diagram for the symmetric-arm model has the same structure of the phase diagram of the original associating lattice gas model. Figure 7 shows the full $\bar{p}$–$\bar{T}$ coexistence lines and the TMD line. The two critical points, at the ends of the gas–LDL and of the LDL–HDL coexistence lines, are shown in comparison with the other models in table 1.

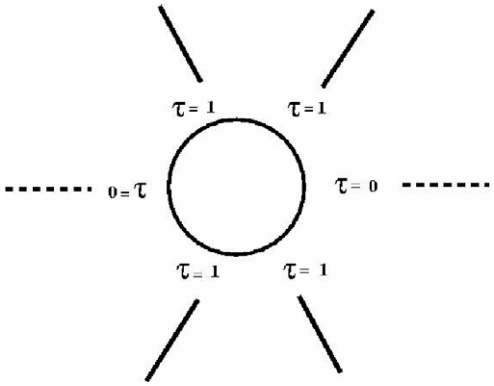

Figure 6. The symmetric model.

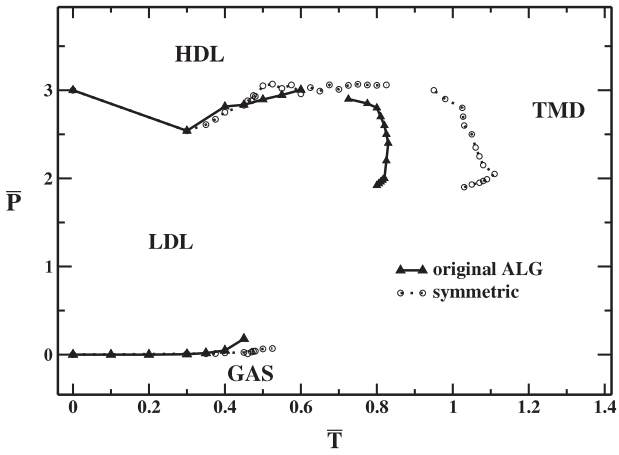

Figure 7. $\bar{p}$–$\bar{T}$ coexistence lines and the TMD line for the symmetric model. The original ALG data are also shown, representing the asymmetric case.

Entropy effects here are the opposite of those found for the distorted-bond model. Hydrogen bonding states have a lower degeneracy, in comparison with the symmetric associating lattice gas model [20, 21]. Accordingly, the critical temperature is increased and the slope of the coexistence curve near the critical point diminishes (see figure 7).

4. H-bond net disruption and density anomaly

The lack of a proton entropy on bonds, in the case of the symmetric-arm model, poses the question of its effect on the behaviour of those bonds, under temperature and pressure variations. We have thus measured the number of hydrogen-bonds per particle over the whole phase diagram, and particularly in the region of the density anomaly. Figures 8(a) and (b) illustrate our findings. The two figures show (a) H-bonds per particle as a function of temperature and (b) density as a function of temperature, at the same pressures. H-bond density decreases as temperature increases at all pressures. However, for those pressures for which a density anomaly is present ($p = 2$ and 2.5), a special behaviour of bonds can be

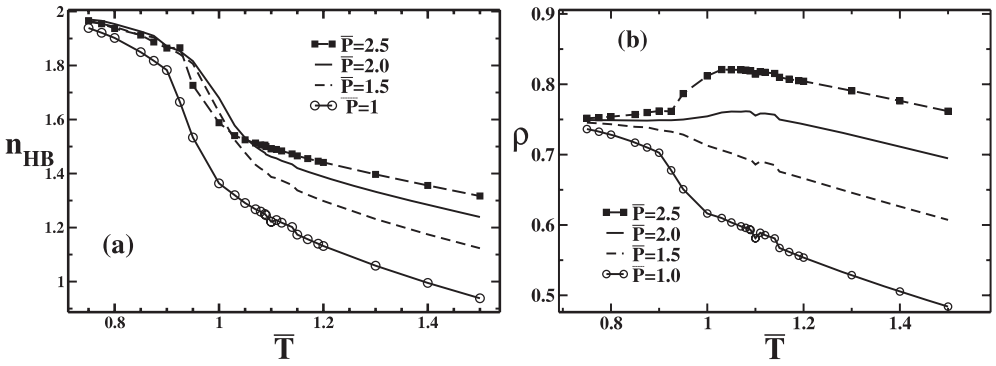

Figure 8. (a) Number of H-bonds per particle versus reduced temperature at fixed reduced pressures. (b) Density versus reduced temperature for fixed pressures.

seen: note the crossings of the isobaric H-bond densities. On the right-hand side of the graph, H-bond numbers increase steadily with pressure. On the left, at lower temperatures, H-bonds may decrease with pressure, as indicated by the crossings. The crossing is a result of the fact that bond breaking is at a much higher rate for $p = 2.5$ than for $p = 1.5$. This result implies a correlation between the behaviour of bonds and of density, in the anomalous region. At the pressures of anomalous density behaviour, a sharp decrease in bond density is seen as the density rises, at the lower temperatures. At the higher temperatures, and for normal density behaviour (which goes down with temperature), H-bond densities decrease steadily with temperature, at all pressures. An interesting picture emerges, confirming and restricting an old qualitative prediction [24]. The increase in density is associated with the disruption of the hydrogen-bond net. However, the *rate* of disruption is important in order to establish the presence of the density increment. If it is too small, the density anomaly is absent.

The coupling of anomalous density and anomalous bond disruption is not restricted to the symmetric-arm model. The behaviour of hydrogen bonds for the other versions of the model, with either distorted bonds or asymmetric (donor–acceptor) arms, are entirely analogous (not shown). In particular, this result implies that, in spite of their presence, distortions may not play an essential role in relation to density anomaly.

5. Conclusions

In this paper we firstly address two questions: (i) what are the effects of distortions of the HB on the density anomaly or on liquid polymorphism and (ii) is the hydrogen distribution entropy on the HB net relevant from the point of view of the characteristic features exhibited by these two properties?

We have investigated these two questions in relation to an associating lattice gas model studied previously. The original model exhibits two liquid phases and a line of density anomalies (TMD). Two features of the phase diagram merit some attention. One of them is the slope of the liquid–liquid coexistence line, which is positive except at low temperatures. This implies that the low-density phase has higher entropy than the high-density phase, contrary to some previous expectations for this line [2]. A second feature is that the liquid–liquid critical temperature is higher than the gas–liquid critical temperature. Although present in other models with liquid polymorphism (albeit without a density anomaly) [25], this feature is contrary to what one would like for a model which describes water.

Could these two features be in any way modified by adding degrees of freedom, present in the real system? Our answer to this question is no. Distortions do not reduce the liquid–liquid critical temperature below the liquid–gas critical temperature and introduce more entropy into the low-density phase.

On the other hand, removing the distinction between donor and acceptor arms, responsible for proton distribution entropy, implies reduction of the number of degrees of freedom and leads to opposite effects on the phase diagram. Our results show that these are the sole important products of either modification: both the gas–liquid and the liquid–liquid critical temperatures, and also the slope of the liquid–liquid line, are re-scaled, while the overall features of the phase diagram remain unaltered.

A second point we were able to establish is the correlation between the rate of H-bond disruption and the presence of a density anomaly. The latter is present only if the rate of bond breaking with increasing temperature is sufficiently high. This property is independent of the presence of bond distortions or of the distinction of acceptor and donor arms. This could be an indication of the greater relevance of bond disruption in relation to bond distortion in the arising of a density anomaly.

Acknowledgments

This work was supported by the Brazilian science agencies Capes, CNPq, FINEP and Fapesp.

References

[1] Debenedetti P G 1998 *Metastable Liquids: Concepts and Principles* (Princeton, NJ: Princeton University Press)
[2] Poole P H, Sciortino F, Essmann U and Stanley H E 1992 *Nature* **360** 324
Poole P H, Sciortino F, Essmann U and Stanley H E 1993 *Phys. Rev.* E **48** 3799
Sciortino F, Poole P H, Essmann U and Stanley H E 1997 *Phys. Rev.* E **55** 727
Harrington S, Zhang R, Poole P H, Sciortino F and Stanley H E 1997 *Phys. Rev. Lett.* **78** 2409
[3] Tanaka H 1996 *J. Chem. Phys.* **105** 5099
Tanaka H 1996 *Nature* **380** 328
[4] Mishima O 2000 *Phys. Rev. Lett.* **85** 334
Mishima O and Suzuki Y 2002 *Nature* **419** 599
[5] Franzese G, Marques M I and Stanley H E 2003 *Phys. Rev.* E **67** 011103
Franzese G and Stanley H E 2002 *Physica* A **314** 508
[6] Sciortino F, La Nave E and Tartaglia P 2003 *Phys. Rev. Lett.* **91** 155701
[7] Glosli J N and Ree F H 1999 *Phys. Rev. Lett.* **82** 4659
[8] Ghiringhelli L M, Los J H, Meijer E J, Fasolino A and Frenkel D 2005 *Phys. Rev. Lett.* **94** 145701
[9] Monaco G, Falconi S, Crichton W A and Mezouar M 2003 *Phys. Rev. Lett.* **90** 255701
[10] Saika-Voivod I, Sciortino F and Poole P H 2001 *Phys. Rev.* E **63** 011202
Saika-Voivod I, Poole P H and Sciortino F 2001 *Nature* **412** 514
[11] Angell C A, Borick S and Grabow M 1996 *J. Non-Cryst. Solids* **207** 463
Poole P H, Hemmati M and Sciotino F 2001 *Nature* **412** 514
[12] Sastry S and Angell C A 2003 *Nat. Mater.* **2** 739
[13] Brazhkin V V *et al* 2002 *New Kinds of Phase Transitions: Transformations in Disordered Susbstances* (*NATO Advanced Research Workshop (Volga River)* vol II/81) ed V Brazhkin, S V Buldyrev, V Ryzhov and H E Stanley (Dordrecht: Kluwer)
[14] Brazhkin V V, Lyapin A G and Tsiok O B 1998 *Rev. High Pressure Sci. Technol.* **7** 347
[15] Hu C-K 1983 *J. Phys. A: Math. Gen.* **16** L321
[16] Attard P 1996 *Physica* A **233** 742
[17] Nadler W and Krausche T 1991 *Phys. Rev.* A **44** R7888
[18] Guisoni N and Henriques V B 2000 *Braz. J. Phys.* **30** 736
[19] Lieb E H 1967 *Phys. Rev. Lett.* **18** 692
[20] Henriques V B and Barbosa M C 2005 *Phys. Rev.* E **71** 031504

[21] Henriques V B, Guisoni N, Barbosa M A, Thielo M and Barbosa M C 2005 *Mol. Phys.* **103** 3001
[22] Patrykiejew A, Pizio O and Sokolowski S 1999 *Phys. Rev. Lett.* **83** 3442
Bruscolini P, Pellizola A and Casetti L 2001 *Phys. Rev. Lett.* **88** 089601
Buzano C, Pellizola A and Pretti M 2004 *Phys. Rev.* E **69** 061502
Silverstein K A T, Haymet A D J and Dill K A 1998 *J. Am. Chem. Soc.* **120** 3166
Truskett T M, Debenedetti P G, Sastry S and Torquato S 1999 *J. Chem. Phys.* **111** 2647
Truskett T M and Dill K A 2002 *J. Chem. Phys.* **117** 5101
[23] Netz P A, Starr F W, Stanley H E and Barbosa M C 2001 *J. Chem. Phys.* **115** 344
[24] Eisenberg D and Kauzmann W 1969 *The Structure and Properites of Water* (Oxford: Clarendon)
[25] Franzese G, Malescio G, Skibinsky A, Buldyrev S V and Stanley H E 2001 *Nature* **409** 692